ACS OMEGA

http://pubs.acs.org/journal/acsodf

Article

Catalytic Activities of Various Niobium Oxides for Hydrogen Absorption/Desorption Reactions of Magnesium

Keita Shinzato, Hiroyuki Gi, Toru Murayama, Masahiro Sadakane, Yongming Wang, Shigehito Isobe, Takayuki Ichikawa, and Hiroki Miyaoka*

Cite This: *ACS Omega* 2021, 6, 23564−23569

Read Online

ACCESS | Metrics & More | Article Recommendations | Supporting Information

ABSTRACT: Five types of niobium(V) oxides (Nb_2O_5) were synthesized by hydrothermal and heat treatment processes, and their structural properties and catalytic activities for the hydrogen absorption/desorption reactions of magnesium were characterized. The synthesized Nb oxides were dispersed on magnesium hydride (MgH_2), a typical hydrogen storage material, using the ball-milling method. All the synthesized Nb oxides improved the reaction kinetics of the hydrogen desorption/absorption reactions. The catalytic activities for the hydrogen desorption were comparable, while the hydrogen absorption rates were significantly different for each synthesized Nb oxide. This difference can be explained by the structural stability of Nb_2O_5, which is related to the formation of a catalytically active state by the reduction of Nb_2O_5 during the ball-milling process. Notably, the highest catalytic effect was observed for Nb_2O_5 with a highly crystalline pyrochlore structure and a low specific surface area, suggesting that pyrochlore Nb_2O_5 is a metastable phase. However, only the amorphous Nb oxide was out of order, even though there is a report on the high catalytic activity of amorphous Nb oxide. This is attributed to the initial condensed state of amorphous Nb oxide, because particle size affects the dispersion state on the MgH_2 surface, which is also important for obtaining high catalytic activity. Thus, it is concluded that Nb_2O_5 with lower stability of the crystal structure and smaller particle size shows better catalysis for both hydrogen desorption and absorption reactions.

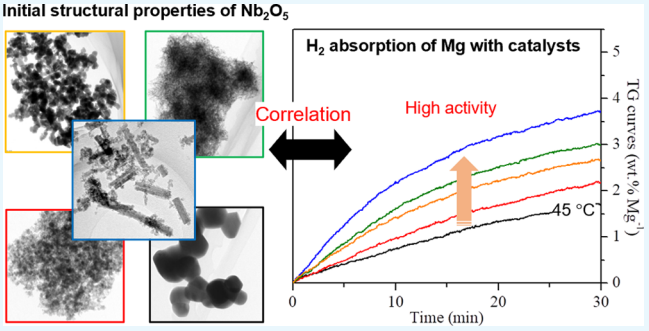

INTRODUCTION

Niobium(V) oxide (Nb_2O_5) has been studied for its use in electrochromic and photoelectrochemical devices[1,2] and catalysis.[3,4] Niobium oxides form different types of crystal structures, such as monoclinic, orthorhombic, pseudohexagonal, and tetragonal. They also exhibit amorphous and pyrochlore structures, which are metastable.[5,6] The structure of Nb oxide strongly depends on the precursors, synthesis methods, and heat-treatment conditions.[6,7] In addition, Nb oxides exhibit different local structures such as distorted octahedral (NbO_6), pentagonal bipyramids (NbO_7), and hexagonal bipyramids (NbO_8).[7] Thus, the synthesis process, structure, and functional properties of Nb_2O_5 have been widely investigated to date.

In the field of hydrogen storage materials, Nb_2O_5 is an excellent catalyst for hydrogen absorption/desorption reactions of magnesium (Mg).[8] Magnesium hydride (MgH_2) has been studied as a hydrogen storage material because of its abundance and high hydrogen storage capacity (7.6 wt %). The main disadvantage of MgH_2 is its slow reaction kinetics for hydrogen desorption and absorption.[9] In particular, the kinetics of the surface reaction, in which hydrogen molecules (H_2) are dissociated and recombined in the hydrogen absorption and desorption processes, respectively, needs to be improved because the Mg surface is not active for H_2 dissociation and recombination. It is well-known that active sites on the surface are required to improve the heterogeneous reaction between solid-state materials and hydrogen. Furthermore, the d orbital electrons in transition-metal catalysts play a major role in the dissociation of hydrogen molecules into atoms. However, Mg itself does not have d electrons, resulting in low H_2 dissociation ability. Thus, thermal activation and high pressure are often required to conduct the reactions of Mg without a catalyst. Therefore, transition metals have been explored as catalysts for Mg.[10,11] Mg mixed with mesoporous Nb_2O_5 can absorb approximately 4 wt % H_2 within 3 h even at −10 °C under 0.2 MPa of H_2, whereas Mg without Nb requires 100 °C and 2.0 MPa of pressure to achieve similar kinetics.[12] It has been reported that Nb_2O_5 is

Received: July 12, 2021
Accepted: August 24, 2021
Published: September 3, 2021

reduced to NbO (Nb^{2+}) on reaction with MgH_2 during ball-milling, and NbO is considered as the active state for the catalysis of hydrogen absorption/desorption reactions of Mg.[13] The chemical and physical properties of initial Nb_2O_5 are considered to affect the oxidation state of Nb after ball-milling. We studied the dependence of the initial state of Nb_2O_5 on hydrogen absorption/desorption of Mg. It was found that, amorphous Nb_2O_5, which is metastable, can be easily converted to an active state compared with crystalline Nb_2O_5.[14] In a recent work, when a Nb oxide was synthesized by the hydrolysis of niobium(V) ethoxide, $Nb(OC_2H_5)_5$, the −OH functional group remained in the synthesized Nb oxide. The −OH group inhibits the formation of Nb−O−Nb linkages, and the Nb oxide without heat treatment shows catalytic effects comparable to those of Mg ball-milled with mesoporous Nb_2O_5 for 20 h for hydrogen absorption/desorption of Mg even in a short-time dispersion process (2 h ball-milling).[15] Thus, the crystal structure and the chemical state strongly affect the active state of Nb. However, the catalytic properties of Nb oxides with other structures have not been investigated yet.

In this work, five types of Nb oxides were synthesized by hydrothermal method and calcination, and the catalytic effects of these oxides on the hydrogen absorption/desorption kinetics of Mg were investigated. From the obtained results, the correlation between the catalytic and structural properties of Nb_2O_5 is discussed.

RESULTS AND DISCUSSION

Five types of Nb_2O_5 were synthesized by using different precursors and methods, and these Nb_2O_5 were denoted as mono-NbO, amor-NbO, pyro-NbO, layered-NbO, and ortho-NbO, respectively, as explained in the experimental section. As shown in Figure 1, the prepared Nb oxides exhibit different powder X-ray diffraction (XRD) patterns corresponding to different crystal structures. The XRD pattern of mono-NbO can be assigned to a mixture of orthorhombic and monoclinic crystal structures. Although two phases are observed in mono-NbO, the monoclinic structure is reportedly the most stable phase.[7] Amor-NbO does not show any diffraction peaks, indicating its amorphous nature. Although the diffraction peaks of pyro-NbO do not match any references shown in Figure 1, the characteristic XRD pattern has been assigned to those originated in the pyrochlore-type structure reported in previous work.[6] Layered-NbO is almost amorphous; however, it has an ordered structure for *c*-axis like layered materials.[6] Therefore, it is speculated that layered-NbO is more stable than the fully amorphous amor-NbO. In addition, the XRD pattern of ortho-NbO, which is synthesized from the same precursor as that of layered-NbO at a higher temperature of 700 °C, shows peaks corresponding to the orthorhombic structure. Therefore, the structural stability of the Nb_2O_5 samples is in the order: mono-NbO > ortho-NbO > layered-NbO > amor-NbO. Pyrochlore Nb_2O_5 has high crystallinity, but it has been reported that the intensities of the XRD peaks decrease below 400 °C.[6] This behavior indicates that the thermal stability of pyrochlore Nb_2O_5 is low. In fact, weight loss due to water desorption was observed during heating up to 400 °C under Ar flow (see Supporting Information, Figure S2). On the other hand, amor-NbO was stable at this temperature because it was prepared by calcination at 400 °C for 2 h, and the water desorption observed in the thermogravimetry−differential thermal analysis (TG−DTA) is very small. Therefore, amor-NbO is more stable than pyro-NbO. Consequently, the thermodynamic stability of the Nb_2O_5 samples is ordered as mono-NbO > ortho-NbO > layered-NbO > amor-NbO > pyro-NbO. Here, although the main composition of synthesized samples would be expressed by Nb_2O_5, some samples include small amount of H_2O and/or −OH groups. Transmission electron microscopy (TEM) observation was carried out to understand the morphology and crystallinity of initial Nb oxides, as shown in Figure 2. Mono-NbO consists of spherical particles with size of approximately 200 nm, as shown in Figure 2a, and interference fringes are observed in the high-resolution TEM image, as shown in Figure 2b. The electron diffraction pattern in the inset of Figure 2b shows clear diffraction spots, which evidences a highly crystalline state. Monoclinic Nb_2O_5 is formed by heating up to 1000 °C,[7] indicating that mono-NbO has high crystallinity and large particle size. Amor-NbO, which was prepared by calcination of $Nb_2O_5{\cdot}nH_2O$ at 400 °C, exhibits a porous structure, as shown in Figure 2c−d. The surface area of amor-NbO estimated by N_2 adsorption measurements was relatively higher than that of the other prepared Nb oxides, as shown in Table 1. Although it is difficult to estimate the particle size because of the unclear interface, several tens of nanometer-sized particles appear to have condensed together. The electron diffraction pattern showed a halo, which is typical of amorphous materials; this result is consistent with that of XRD. For pyro-NbO, pillar-like crystallites are observed (Figure 2e), and the clear diffraction spots and interference fringes, as shown in Figure 2f, indicate its high crystallinity. When the precursor was changed from $Nb_2O_5{\cdot}nH_2O$ to $NH_4[NbO(C_2O_4)_2(H_2O)_2]{\cdot}nH_2O$, the crystal structure and the morphology changed even after being prepared under the same hydrothermal conditions. Ribbon- or fiber-shaped particles are observed in the TEM image of layered-NbO, as shown in Figure 2g−h. Based on previous reports, these particles grow along the *c*-axis and form a layer-like structure.[6] Thus, the peak corresponding to the (001) plane was observed in the XRD pattern of layered-NbO. However, the XRD and electron diffraction patterns are typical of amorphous-like materials, indicating its low crystallinity.

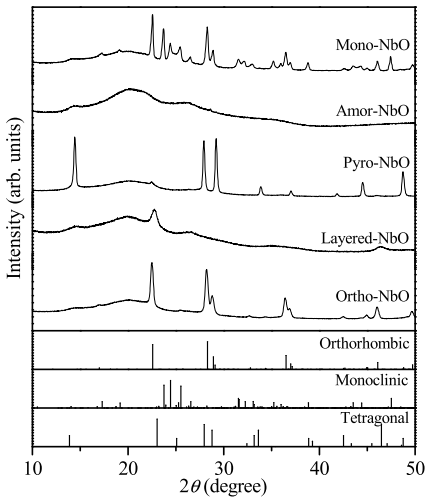

Figure 1. XRD patterns of the synthesized Nb_2O_5. The Nb oxides with orthorhombic (PDF card no. 00-027-1003), monoclinic (PDF card no. 00-037-1468), and tetragonal (PDF card no. 00-018-0911) structures are shown as the references.

https://doi.org/10.1021/acsomega.1c03687
ACS Omega 2021, 6, 23564−23569

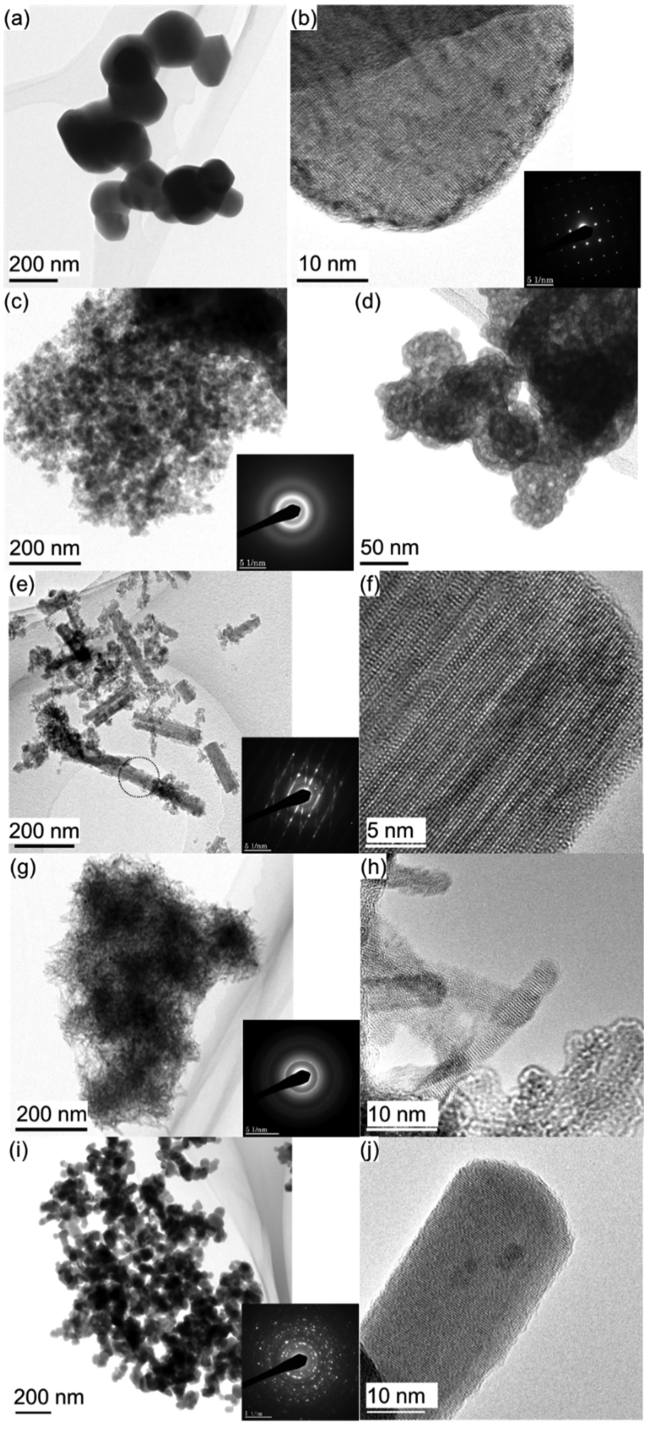

Figure 2. TEM images and electron diffraction patterns of synthesized Nb_2O_5: mono- (a,b), amor- (c,d), pyro- (e,f), layered- (g,h), and ortho- (i,j) NbO.

This indicates that the atomic arrangement in the $a-b$ plane is not in an ordered state. As shown in Figure 2i–j, ortho-NbO is block-shaped, and its crystallinity is relatively high (indicated by the clear electron diffraction spots). The ortho-NbO particles formed a condensed state composed of several tens of nanometer-sized crystallites, similar to amor-NbO. The above results clarify that the five types of Nb oxides possess different structural properties. The crystal structure, morphology, and the results of N_2 adsorption measurements are summarized in Table 1.

To understand the relationship between the initial structural properties and catalysis of Nb_2O_5 for hydrogen absorption/desorption of Mg, TG–DTA–mass spectrometry (MS) measurements of MgH_2 mixed with the synthesized Nb oxides were carried out under 0.1 MPa of Ar and H_2 flows, respectively. The MS and TG profiles of MgH_2 + 1 mol % Nb_2O_5 performed under Ar flow at 5 °C/min are shown in Figure 3. All the samples desorb below 300 °C, which is lower

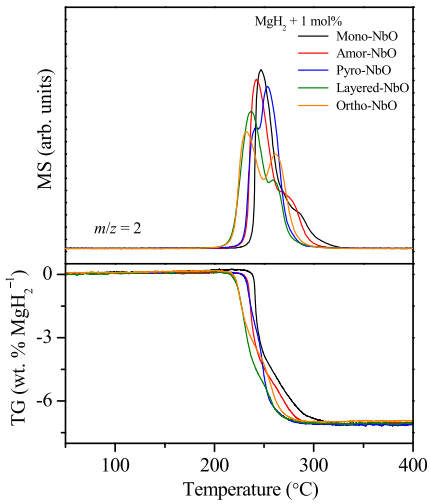

Figure 3. MS and TG curves of the MgH_2 + 1 mol % of each Nb_2O_5. The measurements were carried out under Ar flow at a heating rate of 5 °C/min.

than the temperature for MgH_2 without catalysts and is comparable to the temperature reported in previous works.[16] The weight losses observed by TG analyses correspond to the theoretical hydrogen capacity of MgH_2 + 1 mol % Nb_2O_5, suggesting complete decomposition of MgH_2. The phase change of MgH_2 to Mg was confirmed from XRD analyses (Supporting Information, Figures S3–S7). These results suggest that all the synthesized Nb oxides show catalytic effects for H_2 desorption of MgH_2, even though the initial crystal structure of the Nb oxide was different. Namely, the activation energy of reaction on the Mg surface, which is recombination of hydrogen atoms to form H_2, is reduced as

Table 1. Structural and Morphological Information of Synthesized Nb_2O_5

name	structure	morphology	SSA (m^2/g)[a]	pore volume (cm^3/g)[b]	pore diameter (nm)[b]
mono-NbO	monoclinic tetragonal	spherical crystallites (condensed state)	4	0.04	1.4
amor-NbO	amorphous	porous particles	118	0.23	3.5
pyro-NbO	pyrochlore	pillar crystallites	30	0.09	7.4
layered-NbO	amorphous-like(layered)	ribbon/fibers	205	0.57	1.4
ortho-NbO	orthorhombic	block crystallites	10	0.20	1.4

[a]Estimated by the Brunauer–Emmett–Teller method. [b]Estimated by the Barrett–Joyner–Halenda method.

https://doi.org/10.1021/acsomega.1c03687
ACS Omega 2021, 6, 23564–23569

discussed in previous work.[12] However, it is difficult to compare and discuss the detailed difference in the catalytic properties of all the Nb_2O_5 samples. Although the synthesis time of the Nb_2O_5-dispersed MgH_2 in this work is ten times shorter than that reported in previous studies, the catalysis is not clearly different. This suggests that the catalytically active state is easily formed in all the synthesized Nb_2O_5 samples. In addition, thermal activation effects are also included in the endothermic hydrogen desorption process. Thus, the hydrogen desorption temperature was almost the same for all the samples. Two peaks of H_2 desorption are observed in the MS spectra of all the samples, indicating that the Nb oxides in the samples are intermediates of the catalytically active states. A long ball-milling time is required to form a homogeneous state because ball-milling of two solid materials is a heterogeneous process.[16] In other words, it is considered that the shape of the desorption peak of MgH_2 with Nb prepared under a short milling time strongly depends on the initial state of the Nb oxides. In fact, the peak profiles are different for each sample. The peak temperatures are presented in Table 2. The

Table 2. Peak Temperatures of Hydrogen Desorption and the Amount of Absorbed Hydrogen on the Prepared MgH_2 with Each Nb_2O_5

name	peak temperature of H_2 desorption (°C)	amount of absorbed H_2 (wt %)
mono-NbO	247, 283 (36)	1.7
amor-NbO	242, 273 (31)	2.2
pyro-NbO	242, 253 (11)	3.7
layered-NbO	237, 259 (22)	3.0
ortho-NbO	232, 262 (30)	2.7

difference in the peak temperatures is the smallest for pyro-NbO and largest for mono-NbO. This indicates that a relatively homogeneous active state is formed by the unstable pyro-NbO. However, the peak difference for amorphous amor-NbO is relatively large, although its structural stability is low (discussed before). This may be attributed to the condensed state of amor-NbO, which leads to low dispersion on the MgH_2 surface during short-time milling. As a result, the frequency factor of the catalytic surface reaction would be relatively low compared with that of the high dispersion state. It has been reported that amorphous Nb_2O_5 with a small particle size has higher catalytic activity than that with a large particle size.[14]

Figure 4 shows the hydrogen absorption curve of MgH_2 after the hydrogen desorption measurement. Mg without the catalyst absorbs 1 wt % of H_2 at 60 °C and 2 MPa of H_2 within 100 min.[12] On the other hand, all the prepared samples absorb more than 1 wt % of H_2 at 0.1 MPa of H_2. The XRD results showed formation of MgH_2 in all the samples (see Supporting Information, Figures S3−S7). Therefore, all the synthesized Nb oxides catalyzed the hydrogen absorption of Mg. The hydrogen absorption measurements were carried out at low temperatures, indicating that thermal activation is negligible. Hence, the kinetics of hydrogen absorption is affected only by the catalytic effects of the Nb oxides. The amount of absorbed hydrogen is different in each sample during the reaction for 30 min, as shown in Figure 4 and Table 2. It is worth noting that the amount of hydrogen absorbed increased with decrease in the stability of the Nb oxides (even with different crystal structures); only amor-NbO showed a

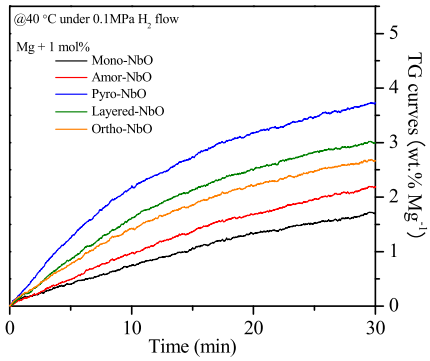

Figure 4. Hydrogen absorption curves of the Mg + 1 mol % of each Nb_2O_5 under 0.1 MPa of H_2 flow around 45 °C.

different trend with lower catalytic activity. This behavior can be explained by the formation of the condensed state (large particle size) as discussed before. Here, we tried to evaluate the dispersion state of Nb oxides. However, it was difficult to distinguish Nb species even by TEM. In fact, it is reported that the catalytic active Nb species is highly dispersed with nano-size on the Mg surface.[17]

The reduction rate of Nb_2O_5 during the ball-milling with MgH_2 depends on the structural stability of Nb_2O_5. In other words, the catalytically active Nb (Nb^{2+}) can be formed easily for the unstable Nb_2O_5. On the other hand, only amor-NbO was out of trend for the crystal stability, and the low dispersion state due to condensation of Nb_2O_5 observed by TEM would be the reason for the lower catalysis. From the above experimental results, it can be understood that the structural stability as well as the particle size of initial Nb_2O_5 are important factors that affect the formation of catalytic active states of Nb_2O_5 for the hydrogen absorption/desorption reactions of MgH_2, whereas the specific surface area is not significant for the catalysis. The pyrochlore-type Nb_2O_5 with low stability and crystalline/particle size revealed the best catalytic performance for Mg.

CONCLUSIONS

In this work, five types of Nb(V) oxides with different structures were synthesized by hydrothermal treatment and calcination. The prepared Nb(V) oxides were characterized by XRD, TEM, and N_2 adsorption measurements. The catalytic activities of the synthesized Nb_2O_5 samples for hydrogen absorption and desorption reactions of Mg were investigated. The crystal structure depended on the precursor, treatment method, and temperature. The XRD results showed that mono-, amor-, pyro-, layered-, and ortho-NbO exhibit monoclinic, amorphous, pyrochlore, amorphous-like layered, and orthorhombic structures, respectively. Comparing the structure with previous reports, the stability of Nb_2O_5 was in the following order: mono-NbO > ortho-NbO > layered-NbO > amor-NbO > pyro-NbO. The shape, condensed state, and crystallinity of Nb_2O_5 were characterized using TEM. A decrease in the peak temperature of hydrogen desorption from MgH_2 was observed in the MS analyses of all the MgH_2 catalyzed by Nb_2O_5. The temperatures are comparable with those reported previously, and the peak temperature was almost the same for all the prepared Nb_2O_5 samples. Peak splitting due to the low homogeneity of the catalytic active states was observed. Among all the samples, pyro-NbO was more homogeneously transformed into a catalytically active

https://doi.org/10.1021/acsomega.1c03687
ACS Omega 2021, 6, 23564−23569

state. The synthesized Nb_2O_5 shows obviously different catalytic effects on hydrogen absorption by Mg. The reaction kinetics of hydrogen absorption improved with decreasing structural stability of Nb_2O_5, excluding amor-NbO (which may be attributed to its condensed state). From the above experimental results, it is concluded that structural properties such as stability and particle size of initial Nb_2O_5 affect the formation of the catalytically active state for hydrogen absorption and desorption reactions by MgH_2.

EXPERIMENTS

Five types of Nb_2O_5 with different structures and morphologies were prepared by calcination and hydrothermal methods to understand the effects of the initial state of Nb_2O_5 on the hydrogen absorption and desorption of Mg. Nb_2O_5 (reference no. JRC-NBO2) and niobium oxide hydrate ($Nb_2O_5{\cdot}nH_2O$, reference no. JRC-NBO1) were provided by Catalysis Society of Japan. These Nb oxides were calcined at 400 °C for 2 h in air. The Nb oxides of JRC-NBO2 and JRC-NBO1 after calcination are denoted as mono-NbO and amor-NbO, respectively. Pyrochlore niobium oxide and layered-structure-type niobium oxide were synthesized by the hydrothermal method from niobic acid ($Nb_2O_5{\cdot}nH_2O$, Soekawa Chemical) and ammonium niobium oxalate ($NH_4[NbO(C_2O_4)_2(H_2O)_2]{\cdot}nH_2O$, CBMM), respectively. To synthesize pyrochlore niobium oxide, hydrothermal treatment was carried out at 175 °C for 72 h. The sample was then calcined at 300 °C for 2 h in air. This sample is denoted as pyro-NbO. For the layered-structure-type niobium oxide, the hydrothermal treatment was carried out at the same temperature for 24 h. Then, the sample was calcined at 400 and 700 °C, and the obtained Nb oxides are denoted as layered-NbO and ortho-NbO, respectively. The details of the hydrothermal synthesis are described in our previous report.[6] All the synthesized Nb oxides were heated at 200 °C for 8 h under dynamic vacuum to remove adsorbed impurity gases and transferred into a glove box (Miwa MFG, MDB-2BL) filled with high purity Ar (>99.9999%). To investigate the catalytic effects of the Nb oxides on the hydrogen absorption/desorption reactions of Mg, MgH_2 was mixed with 1 mol % of each Nb oxide. The number of moles of Nb oxide was calculated by assuming the formula to be Nb_2O_5. A total of 300 mg of each mixture was ball-milled using a planetary ball-milling apparatus (Fritsch P7) for 2 h at 370 rpm and 1 MPa H_2. A milling pot (30 cm^3) and 20 stainless steel balls (SUJ-2, 7 mm in diameter) were used for the ball-milling. The milling process was stopped for 30 min after 1 h of operation to avoid temperature increase in the milling pot. Here, the ball-milling method is chosen as the dry synthesis process to understand the essential catalytic properties of the Nb oxides without the variation of the Mg surface such as formation of oxide layers. To investigate the hydrogen desorption properties of MgH_2 ball-milled with the Nb oxides, TG−DTA−MS (TG−DTA; Rigaku TG8120, MS; Anelva, M-QA200TS) was carried out under an Ar flow of 0.1 MPa up to 400 °C at a heating rate of 5 °C/min. Here, the mass numbers corresponding to gases such as H_2O and CO_2 expected from the sample synthesis processes are also measured to know other gas emission. The TG−DTA apparatus was also used to measure the hydrogen absorption properties after the dehydrogenation of the MgH_2 samples. After cooling the dehydrogenated sample, it was heated to 35 °C under Ar flow, and then, the carrier gas was switched to 0.1 MPa H_2 at 35 °C. The temperature was maintained for 30 min after the gas change to measure the hydrogen absorption curves. The hydrogen absorption test was performed several times to confirm the repeatability of the catalytic activity for each Nb oxide. Here, although the temperature was slightly increased during the hydrogen absorption measurement due to the exothermic reaction (see Supporting Information, Figure S1), its effect for the hydrogen absorption kinetics of Mg is negligible because the difference is small and there is no tendency with hydrogen absorption properties. The characterizations of the synthesized Nb oxides and MgH_2 ball milled with the Nb oxides were carried out using XRD (Rigaku, RINT 2500V, Cu Kα: 1.54 Å), TEM (JEOL, JEM-2010), and N_2 adsorption measurements (BELSORP-max, BEL Japan). The MgH_2 samples were covered with a polyimide film (Kapton, Du Pont-Toray Co. Ltd.) during XRD measurements to minimize the influence of oxidation.

ASSOCIATED CONTENT

Supporting Information

The Supporting Information is available free of charge at https://pubs.acs.org/doi/10.1021/acsomega.1c03687.

Temperature transition during the TG measurements under H_2 flow, TG−MS results of Nb oxides, and XRD results of MgH_2 with each synthesized Nb oxide in each treatment (PDF)

AUTHOR INFORMATION

Corresponding Author

Hiroki Miyaoka − *Natural Science Center for Basic Research and Development, Hiroshima University, Higashi-Hiroshima 739-8530, Japan; Graduate School of Advanced Science and Engineering, Hiroshima University, Higashi-Hiroshima 739-8527, Japan;* orcid.org/0000-0002-8480-7308; Email: miyaoka@hiroshima-u.ac.jp

Authors

Keita Shinzato − *Natural Science Center for Basic Research and Development, Hiroshima University, Higashi-Hiroshima 739-8530, Japan*

Hiroyuki Gi − *Graduate School of Advanced Science and Engineering, Hiroshima University, Higashi-Hiroshima 739-8527, Japan*

Toru Murayama − *Research Center for Hydrogen Energy-based Society, Tokyo Metropolitan University, Tokyo 192-0397, Japan; Yantai Key Laboratory of Gold Catalysis and Engineering, Shandong Applied Research Center of Gold Nanotechnology (Au-SDARC), School of Chemistry & Chemical Engineering, Yantai University, Yantai 264005, China;* orcid.org/0000-0001-5105-3290

Masahiro Sadakane − *Graduate School of Advanced Science and Engineering, Hiroshima University, Higashi-Hiroshima 739-8527, Japan;* orcid.org/0000-0001-7308-563X

Yongming Wang − *Creative Research Institution, Hokkaido University, Sapporo 001-0021, Japan*

Shigehito Isobe − *Graduate School of Engineering, Hokkaido University, Sapporo 060-8628, Japan*

Takayuki Ichikawa − *Natural Science Center for Basic Research and Development, Hiroshima University, Higashi-Hiroshima 739-8530, Japan; Graduate School of Advanced Science and Engineering, Hiroshima University, Higashi-Hiroshima 739-8527, Japan;* orcid.org/0000-0003-3425-8758

https://doi.org/10.1021/acsomega.1c03687
ACS Omega 2021, 6, 23564−23569

Complete contact information is available at:
https://pubs.acs.org/10.1021/acsomega.1c03687

Author Contributions

The manuscript was written through contributions of all authors. All authors have given approval to the final version of the manuscript.

Notes

The authors declare no competing financial interest.

■ ACKNOWLEDGMENTS

We would like to thank the Center for Functional Nano Oxide at Hiroshima University, International Network on Polyoxometalate Science and JSPS Core-to-Core Program for financial support. The authors are thankful to Prof. Yoshitsugu Kojima for useful discussions and experimental support.

■ REFERENCES

(1) Llordés, A.; Garcia, G.; Gazquez, J.; Milliron, D. J. Tunable Near-Infrared and Visible-Light Transmittance in Nanocrystal-in-Glass Composites. *Nature* **2013**, *500*, 323−326.
(2) Wu, J.; Li, J.; Lü, X.; Zhang, L.; Yao, J.; Zhang, F.; Huang, F.; Xu, F. A One-Pot Method to Grow Pyrochlore $H_4Nb_2O_7$-Octahedron-Based Photocatalyst. *J. Mater. Chem.* **2010**, *20*, 1942−1946.
(3) Zhao, Y.; Zhou, X.; Ye, L.; Chi Edman Tsang, S. Nanostructured Nb_2O_5 Catalysts. *Nano Rev.* **2012**, *3*, 17631.
(4) Chai, S.; Wang, H.; Liang, Y.; Xu, B. Sustainable Production of Acrolein: Gas-Phase Dehydration of Glycerol over Nb_2O_5 Catalyst. *J. Catal.* **2007**, *250*, 342−349.
(5) Ikeya, T.; Senna, M. Change in the Structure of Niobium Pentoxide Due to Mechanical and Thermal Treatments. *J. Non-Cryst. Solids* **1988**, *105*, 243−250.
(6) Murayama, T.; Chen, J.; Hirata, J.; Matsumoto, K.; Ueda, W. Hydrothermal Synthesis of Octahedra-Based Layered Niobium Oxide and Its Catalytic Activity as a Solid Acid. *Catal. Sci. Technol.* **2014**, *4*, 4250−4257.
(7) Jehng, J. M.; Wachs, I. E. Structural Chemistry and Raman Spectra of Niobium Oxides. *Chem. Mater.* **1991**, *3*, 100−107.
(8) Barkhordarian, G.; Klassen, T.; Bormann, R. Fast Hydrogen Sorption Kinetics of Nanocrystalline Mg Using Nb_2O_5 as Catalyst. *Scr. Mater.* **2003**, *49*, 213−217.
(9) Oelerich, W.; Klassen, T.; Bormann, R. Metal Oxides as Catalysts for Improved Hydrogen Sorption in Nanocrystalline Mg-Based Materials. *J. Alloys Compd.* **2001**, *315*, 237−242.
(10) Hanada, N.; Ichikawa, T.; Fujii, H. Catalytic Effect of Nanoparticle 3d-Transition Metals on Hydrogen Storage Properties in Magnesium Hydride MgH_2 Prepared by Mechanical Milling. *J. Phys. Chem. B* **2005**, *109*, 7188−7194.
(11) Liang, G.; Huot, J.; Boily, S.; Van Neste, A.; Schulz, R. Catalytic Effect of Transition Metals on Hydrogen Sorption in Nanocrystalline Ball Milled MgH_2-Tm (Tm=Ti, V, Mn, Fe and Ni) Systems. *J. Alloys Compd.* **1999**, *292*, 247−252.
(12) Kimura, T.; Miyaoka, H.; Ichikawa, T.; Kojima, Y. Hydrogen Absorption of Catalyzed Magnesium below Room Temperature. *Int. J. Hydrogen Energy* **2013**, *38*, 13728−13733.
(13) Hanada, N.; Ichikawa, T.; Isobe, S.; Nakagawa, T.; Tokoyoda, K.; Honma, T.; Fujii, H.; Kojima, Y. X-Ray Absorption Spectroscopic Study on Valence State and Local Atomic Structure of Transition Metal Oxides Doped in MgH_2. *J. Phys. Chem. C* **2009**, *113*, 13450−13455.
(14) Gi, H.; Shinzato, K.; Balgis, R.; Ogi, T.; Sadakane, M.; Wang, Y.; Isobe, S.; Miyaoka, H.; Ichikawa, T. Effective Factor on Catalysis of Niobium Oxide for Magnesium. *ACS Omega* **2020**, *5*, 21906−21912.
(15) Singh, P. K.; Gi, H.; Shinzato, K.; Katagiri, K.; Miyaoka, H.; Ichikawa, T.; Kojima, Y. Synthesis of Highly Activated Magnesium by Niobium and Tantalum Gel Oxide Catalyst. *Mater. Trans.* **2021**, *62*, 284−289.
(16) Hanada, N.; Ichikawa, T.; Fujii, H. Catalytic Effect of Ni Nano-Particle and Nb Oxide on H-Desorption Properties in MgH_2 Prepared by Ball Milling. *J. Alloys Compd.* **2005**, *404−406*, 716−719.
(17) Hanada, N.; Hirotoshi, E.; Ichikawa, T.; Akiba, E.; Fujii, H. SEM and TEM Characterization of Magnesium Hydride Catalyzed with Ni Nano-Particle or Nb_2O_5. *J. Alloys Compd.* **2008**, *450*, 395−399.